DOI:10.22337/2587-9618-2025-21-2-99-115

# STRUCTURAL BEHAVIOR OF GFRP-CONCRETE COMPOSITE COLUMNS UNDER AXIAL LOAD

***Mohammed. A.M. Khalil, Mohammed M. Salem, Ata El-Kariem Shoeib, Alaa Gamal Sherif***

Civil Department, Faculty of Engineering, Mataria, Helwan University, EGYPT

**Abstract**: Glass Fiber Reinforced Polymer (GFRP) is emerging as an effective alternative to traditional steel in construction due to its superior ability to withstand high loads, light weight, corrosion resistance and low maintenance costs. Optimizing the design of GFRP I-section can lead to significant savings construction costs. The main objective of this study is to understand the effect of introducing GFRP I-section internally on the load bearing capacity of Reinforced Concrete (RC) columns with and without fire. Four RC-column specimens were tested with a square cross-section of 160 mm side dimension and 1540 mm height. I-shaped GFRP section with 5.5 mm thickness for web and flanges, 80 mm flange width, and 100 mm total height is fixed in the center of section of column specimens .The specimens are divided into two groups. The first group has two conventional RC tested column specimens which one exposed to the fire 500°C for 90 minutes and the other without fire. The second group has two RC columns specimens reinforced with GFRP I-section which one exposed to the fire 500°C for 90 minutes and the other without fire. This study has shown that GFRP I-section composite columns exhibit excellent strength and high resistance to axial load than the conventional reinforced concrete columns. The maximum bearing capacity for the composite columns with (GFRP) I-section increased 17% more than the conventional RC columns. The maximum bearing capacity for the composite columns with (GFRP) I-section under the fire decreased 39% more than the composite (GFRP) columns without the fire, and decreased 14% more than the conventional RC columns. By different codes the theoretical axial load is calculated for tested specimens. The Finite element analysis was used to verify experimental results for studying additional parameters are the effect of concrete compressive strength, the steel yield strength, the reinforcement ratio, and the GFRP plate and I-section ratio of RC composite columns.

**Keywords:** GFRP I-Section, Composite columns, Reinforced concrete columns, Fire, Analysis, Experimental results, theoretical study, Finite element modelling

# НЕСУЩАЯ СПОСОБНОСТЬ ЖЕЛЕЗОБЕТОННЫХ КОЛОНН, АРМИРОВАННЫХ GFRP - ПРОФИЛЕМ, ПРИ ДЕЙСТВИИ ПРОДОЛЬНОЙ СИЛЫ И ОГНЕВОМ ВОЗДЕЙСТВИИ

***Мохаммед. А.М. Халил, Мохаммед М. Салем, Ата Эль-Карим Шойиб, Алаа Гамаль Шериф***

Кафедра гражданского строительства, инженерный факультет, Матария, Университет Хелуан, ЕГИПЕТ

**Аннотация**: Полимер, армированный стекловолокном (GFRP), является эффективной альтернативой традиционной стали в строительстве благодаря своей способности выдерживать высокие нагрузки при небольшом собственном весе, коррозионной стойкости и низких расходах на эксплуатацию. Оптимизация конструкции двутаврового сечения из GFRP может привести к значительной экономии затрат на строительство. Основной целью данного исследования являлось изучение влияния жесткой арматуры в виде двутавоа, выполненного из GFRP, на несущую способность железобетонных колонн при высокотемпературном воздействии от пожара и без него. Были испытаны четыре образца железобетонных колонн квадратного сечения со стороной 160 мм и высотой 1540 мм. В середине сечения образцов колонн были помещены двутавры из GFRP с толщиной полки и стенки 5,5 мм, шириной полки 80 мм и общей высотой 100 мм. Образцы были разделены на две группы. Первая группа состояла из двух обычных образцов железобетонных колонн, один из которых подвергался огневому воздействию при температуре 500°C в течение 90 минут, а другой не подвергался высокотемпературному воздействию. Вторая группа состояла из двух образцов колонн, армированных двутаврами из GFRP, один из которых подвергался воздействию огня при температуре 500°C в течение 90 минут, а другой не подвергался высокотемпературному воздействию. Данное исследование показало, что колонны, армированные двутаврами из GFRP композита, обладают более высокой прочностью и высокой устойчивостью при сжатии по сравнению с обычными железобетонными колоннами. Максимальная несущая способность колонн, армированных двутаврами из GFRP, увеличилась на 17% по сравнению с обычными железобетонными колоннами. Максимальная несущая способность колонн, армированных композитными двутаврами из GFRP, при воздействии пожара снизилась на 39% по сравнению с аналогичными образцами, не подверженными огневым воздействиям, и оказалась на 14% меньше, чем для обычных железобетонных колонн. В соответствии с различными нормами проектирования выполнен расчет несущей способности испытанных образцов. Для исследования влияния прочности бетона на сжатие, предела текучести стали, процента армирования стальной и GFRP арматурой на несущую способность колонн было дополнительно выполнено моделирование методом конечных элементов.

**Keywords:** Двутавр из GFRP, композитные колонны, железобетонные колонны, пожар, анализ, экспериментальные результаты, теоретическое исследование, метод конечных элементов

## Notation:

$A_{ft}$ Total cross-sectional area of GFRP I-section
$Ag$ Gross area of the concrete column
$A_{st}$ Total cross-sectional area of longitudinal reinforcement
$E_s$ Modulus of elasticity of steel
$f$ Stress at any strain $\varepsilon$
$f_c'$ Ultimate cylinder compressive strength for concrete
$f_{cu}$ Compressive strength of concrete
$f_s$ Stress in steel bars when the concrete reaches the maximum strength
$f_f$ Ultimate compressive strength of GFRP I-section
$f_u$ Ultimate tensile strength of steel
$f_y$ Yield strength of steel
$P_n$ Axial load at the maximum
$\alpha_1$ Ratio of average stress in rectangular compression block to the specified concrete strength
$\varepsilon_c$ Strain in the concrete at reaching the maximum strength
$\eta$ Reduction factor for the high strength concrete for the rectangular stress distribution
$\phi_c$ Resistance factor for concrete and equal to 1.0 for laboratory conditions
$\phi_s$ Resistance factor for steel and equal to 1.0 for laboratory conditions
$\varepsilon_o$ Strain at the ultimate cylinder compressive strength $f_c'$

## 1. INTRODUCTION

The Study of structural behavior of GFRP composite columns under axial load is important in civil engineering due to the recent increase in the use of composite materials in construction. Glass Fiber Reinforced Polymer (GFRP) columns offer advantages such as high strength-to-weight ratio, corrosion resistance, and durability. When combined with concrete, these columns can provide increased load- bearing capacity and ductility compared to traditional RC columns. Research has presented that the behavior of GFRP-concrete composite columns is influenced by factors such as the type and ratio of GFRP, the bond between GFRP and concrete and the GFRP confinement provided in the structure members. Understanding the performance of these composite columns is essential for designing safe and efficient structures that meet modern engineering standards. Further research is needed to optimize design guidelines and improve our understanding of how these innovative materials behave under different loading conditions. Therefore, optimization of the design of composite sections incorporating GFRP can lead to substantial saving in the construction cost. There are many previous studies that have been conducted on the behavior of composite columns reinforced with

GFRP I-profile and steel bars under axial load. Muhammad et al. [1], studied the performance of the behavior of the composite columns reinforced with the GFRP I-section and C-section under axial land eccentric load. The experiments were conducted using an axial compression test and an eccentric compression test with varying eccentricities. The experimental results show that the specimens reinforced with GFRP I-profiles achieved a higher ultimate load but lower ductility in comparison with the reference columns reinforced with steel bars as well as the composite columns reinforced with C-sections. Jing C [2] conducted an experimental and numerical study of reinforced concrete-filled square GFRP tubular columns under axial compression. Muhammad et al. [3], conducted an experimental study on the axial compressive behavior of GFRP tube reinforced concrete columns. The results of the experiments show that the use of GFRP tubes increases the ductility and strength of concrete columns. Tomblin and Barbero [4] investigated the local buckling behavior of on short columns made of GFRP I-sections and reported that they were dominated by local buckling, while Zureick and Scott [5] concluded that global buckling is the failure mechanism for long columns. Zouheir A. Hashem [6] conducted an analytical and experimental studied the behavior of short and long GFRP composite columns. Lei X [7] conducted a representative experimental investigation on the performance of slender (GFRP) square hollow columns subjected to both axial and eccentric loading. Srinath T [8] conducted an experimental and numerical investigation on the bonding and buckling behavior of GFRP circular column under axial compression. Yujun Qi [9] studied the behavior of pultruded glass fiber reinforced polymer GFRP-wood composite columns under axial compression. Aydin [10] conducted an experimental study to evaluate the tensile and compressive strength of the GFRP profiles at 13 different temperatures. The tensile and compressive strengths decreased by 28% and 75%, respectively at 100°C, compared to 25°C. When the temperature reached 200°C, the GFRP profiles had lost about 50% of their tensile strength and all of their compressive strength. This is mainly due to the degradation and softening of the polymer matrix within the GFRP components at high temperatures, resulting in reduced load carrying capacity. In addition, exposure to fire causes thermal expansion mismatches between the GFRP and concrete layers, inducing cracking and delamination effects that further weaken the overall performance of these composite columns. In general, GFRP profiles are very sensitive to high temperatures and relatively stable at low temperatures. Therefore, more attention should be paid to fire performance when GRP profiles are used in a high-temperature environment. In this study, the behavior of composite columns reinforced with GFRP I-section and exposed to fire at a temperature of 500 degrees for 90 minutes is investigated. The results of experimental, theoretical, and numerical models by using finite element analysis study concerning the axial load behavior of GFRP-concrete composite columns are presented. In addition, a practical guideline of composite columns reinforced with GFRP I-section leading to the most economical design is established and presented. All column specimens were tested under axial loading. Based on the experimental and numerical results, the load-strain curves and the failure modes are analyzed.

## 2. EXPERIMENTAL PROGRAM

The experimental study of this research is based on testing the behavior of GFRP-concrete composite columns under axial load. The column samples are shown schematically in Fig. 1, and they consist of the following:

### 2.1 Test parameters and specimen details

Two main parameters are considered, namely the effect of GFRP I-section on the behavior of RC composite columns and the effect of fire. The concrete dimensions and reinforcement details of the tested columns are given in Table 1 and Fig. 1. A total of four specimens were fabricated and tested in this experimental study. All tested columns had an overall height of 1540 mm and a cross section of 160 mm x160 mm. All tested columns were reinforced with longitudinal four steel bars of 10 mm diameter and the steel transverse stirrups of 8 mm diameter at 100 mm spacing. The GFRP I-section is 100 mm total height, 80 mm flange width and 5.5mm thickness of web and flanges for the central placement within the RC composite columns. All of the specimens had the same concrete cover of 15 mm.

*Table 1. Designations of tested columns*

| Specimens | Dim. (mm) | | Steel | | Fire | GFRP I-sec | Notes |
|---|---|---|---|---|---|---|---|
| | h | b | Longitudinal | Stirrups | | | |
| RCC | 1540 | 160 | 4R10 | R8@100 | ---- | ---- | Reference for (RCCGI-C & RCC-F) |
| RCCGI-C | 1540 | 160 | 4R10 | R8@100 | ---- | In center | As comparison for (RCC)<br>The Reference for (RCCGI-C-F) |
| RCC-F | 1540 | 160 | 4R10 | R8@100 | Fire | ---- | As comparison for (RCC) |
| RCCGI-C-F | 1540 | 160 | 4R10 | R8@100 | Fire | In center | As comparison for (RCCGI-C) |

Note that:
RCC: The tested conventional reinforced concrete column,
GI : The GRPR I-section
C : Center position
F : Fire

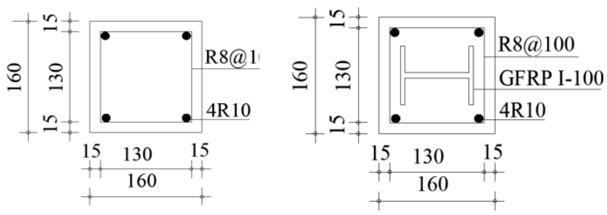


(a) RCC and RCC-F (b) RCCGI-C and RCCGI-C-F

Figure 1. Specimens details of tested column

## 2.2 Material properties

The concrete used was made of Cement (Sina Cement Company), natural siliceous sand, crushed dolomite coarse aggregate with a maximum size of 12.5 mm and superplasticizer (2% of the cement weight). The characteristic compressive strength of the standard concrete cubes after 28 days was 46 MPa. The yield strength and ultimate strength of 8 mm steel bars were 316 MPa and 431 MPa respectively. The yield strength and ultimate strength of 10 mm steel bars were 482 MPa and 652 MPa respectively. According to manufacturing, the tensile strength of GFRP I-section was 336 MPa, and the tensile modulus was 35.3 GPa [11].

## 2.3 Test Setup and Instrumentation

The test frame shown in Fig. 2 was fixed to the strong solid floor of the RC laboratory at the Faculty of Engineering of Helwan University. The supporting setup consisted of a horizontal frame made of four steel I-beams. It was supported by four vertical steel I-beam legs installed on the strong solid floor and the tested columns were rested on the frame. Loading was achieved by using a 1250 kN capacity cell that transferred the axial load to a steel plate with high rigidity/stiffness at the top of the columns, set up as shown in the side part of Fig. 2.
The load was measured by a load cell with 1250 kN capacity which was connected to a digital display unit. The horizontal sway and vertical displacement at the points shown in Fig. 3a were measured using two linear variable differential transducers (LVDTs) and two dial gauges (DGs) with accuracy of 0.01mm. The (LVDTs) and (DGs) were placed on the side and top surface of the columns as shown in Fig. 3b. Four electrical strain gauges were used to measure the strain in the steel bars and GFRP I-section at the maximum tensile point of the steel bars and GFRP I-section as shown in Fig. 4. This location was maintained for all tested columns.

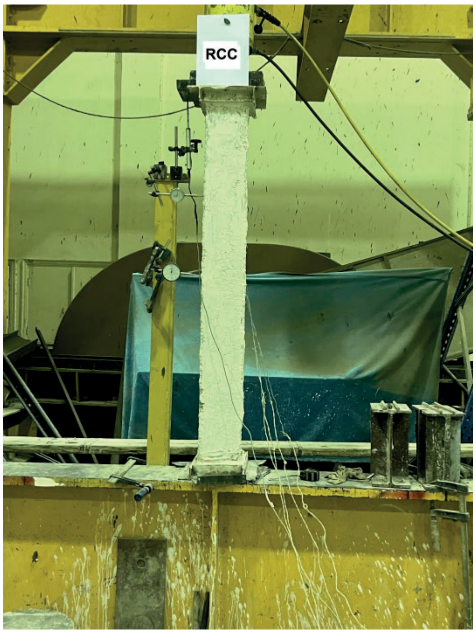


Figure 2. Axial load that transfer from load cell to columns

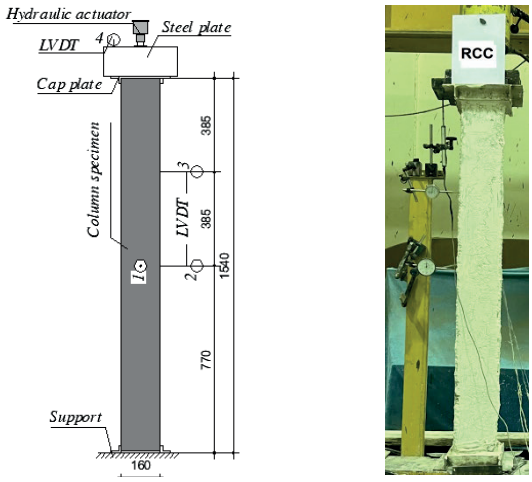


(a) Position (b) Arrangement

Figure 3. Dial gauges and LVDTs

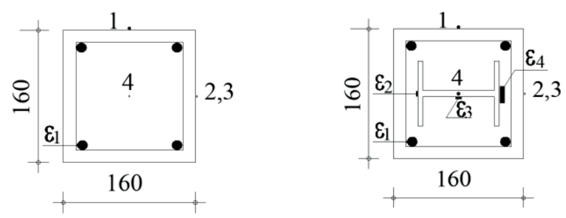


(a) Conventional column (b) Composite columns

Figure 4. Test setup LVDT, DG and strain gauges of columns

## 2.4 Procedure for Firing

The RC column specimens were placed in a circular steel frame with side holes through which the fire was ignited and the specimens were exposed to a fire of 500°C for 90-minutes as shown in Fig. 5. Then the RC columns were left at room temperature for more than 4 hours before loading to failure.


(a) During the fire (b) After the fire

Figure 5. Fire of column specimens

# 3. RESULTS AND DISCUSSION

## 3.1 Failure modes of columns

The failure modes of the columns of all tested specimens are clearly shown in Fig. 6. All the tested specimens failed happened of the concrete in compression failure under axial load and splitting in the reinforcing steel bars, which occurred after the concrete reached its ultimate stress value. In addition, collapse occurred in GFRP I-section flanges for tested RC composite column as shown in Fig. 6b. The failure happened of the concrete at the mid height of the column as there was deterioration in the polymers when exposed to fire because the organic resin matrix used in GFRP I-section compounds is flammable for tested RC composite column with firing as shown in Fig. 6d.

Cracking of the columns started at loads reached more than 83%, and 94% of the maximum load for the reinforced concrete columns without firing and with firing respectively.

*(a) RCC*

*(b) RCCGI-C*

*(c) RCC-F*

*(d) RCCGI-C-F*

*Figure 6. Failure modes of tested columns*

## 3.2 Cracking and maximum load

The cracking and maximum loads are summarized in Table 2. The results show that the composite RC columns achieved 117% of the axial load bearing capacity of the conventional RC columns. The conventional RC columns exposed to firing achieved 86% of the capacity compared to the RC columns without firing. While, the RC composite columns exposed to firing achieved 61% of the capacity comparing RC composite columns without firing due to the organic resin matrix used in GFRP compounds is flammable. The results shown in Fig. 7 indicate that the maximum bearing capacity was achieved in RC composite column. The maximum reduction in column bearing capacity was due to firing at the composite GFRP I-profile column.

*Table 2. The experimental results*

| Specimens | Cra. Load (kN) | Max. Load (kN) | $P_{cr}/P_u$ | $P_u/P_{uCtrl}$ | Notes |
|---|---|---|---|---|---|
| RCC | 996.24 | 1052.90 | 94.62 | 1.00 | Reference for (RCCGI-C & RCC-F) |
| RCCGI-C | 1165.46 | 1234.30 | 94.42 | 1.17 | As comparison for (RCC) Reference for (RCCGI-C-F) |
| RCC-F | 766.30 | 900.71 | 85.08 | 0.86 | As comparison for (RCC) |
| RCCGI-C-F | 621.73 | 746.99 | 83.23 | 0.61 | As comparison for (RCCGI-C) |

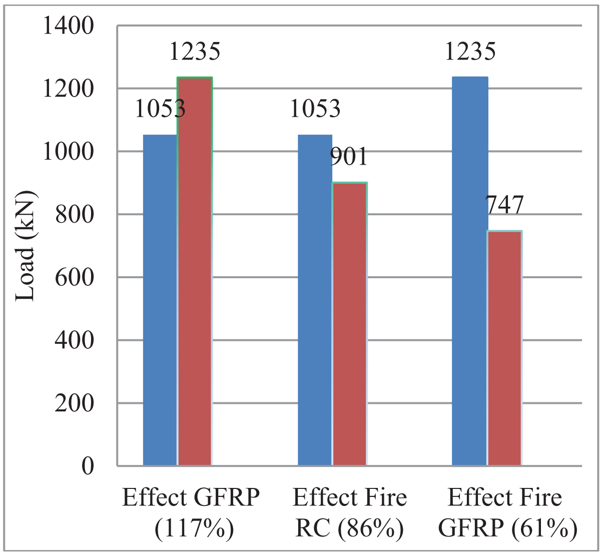


*Figure 7. The maximum load and comparison between of tested columns*

Comparing the maximum loads of the tested columns, it can be noted that the maximum load of the RC composite columns without firing was higher than that of the conventional RC columns. In RC composite columns, the maximum load increased to 117% compared to conventional RC columns.

**3.3 Load–displacement curves**

The load–vertical displacement relationships for the tested conventional and RC composite columns are shown in Fig. 8. The displacement values are those measured at the top height point of the RC columns.

The axial stiffness of the tested columns is the resistance of the columns to deflection or deformation under axial load. Stiffness is defined as the ratio of ultimate load to ultimate deflection [12]. The axial stiffness of conventional RC columns without firing was higher than that of RC composite columns and equal to 131.61 kN/mm and 85.94 kN/mm respectively. The axial stiffness of the tested columns without firing was higher than RC columns with firing, the axial stiffness equal to 131.61 kN/mm and 80.27 kN/mm of conventional RC columns without and with firing respectively, while the axial stiffness equal to 85.94 kN/mm and 59.52 kN/mm of RC composite columns without and with firing respectively because of the large deformation.

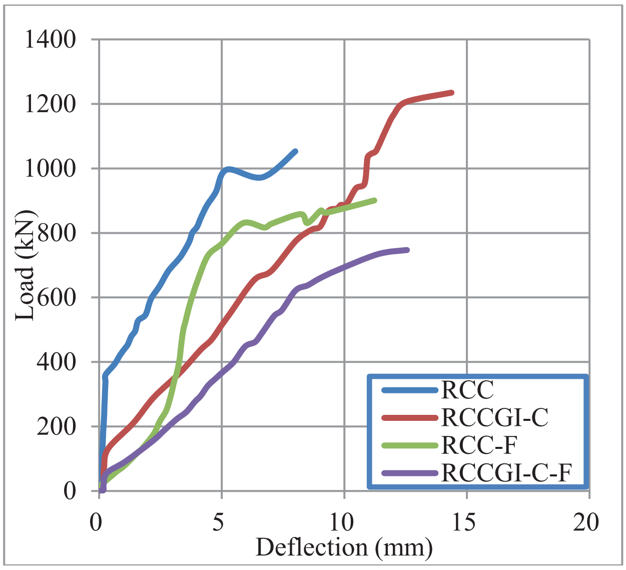


*Figure 8. Load vertical displacement curves of tested columns*

The comparison between the conventional RC columns and the RC composite columns without firing shows that the RC composite columns are more ductile than the conventional RC columns.

**3.4 Stress strain curves**

The measured stress-strain curves of the tested RC composite column without firing are shown in Fig. 9. The axial strain in steel bars and GFRP I-section has similar behavior at the same load level and recorded low strains of the tested column without firing, while the transverse strain in GFRP I-section is a small value compared to the axial strain. In general, the maximum strain in the steel bars and GFRP I-section not reached half the yielding strain of steel bars. Fig. 9 of RC composite column shows that the strain compatibility in deflection both internal steel and GFRP materials within the columns experience similar strains and deformations when subjected to axial load.

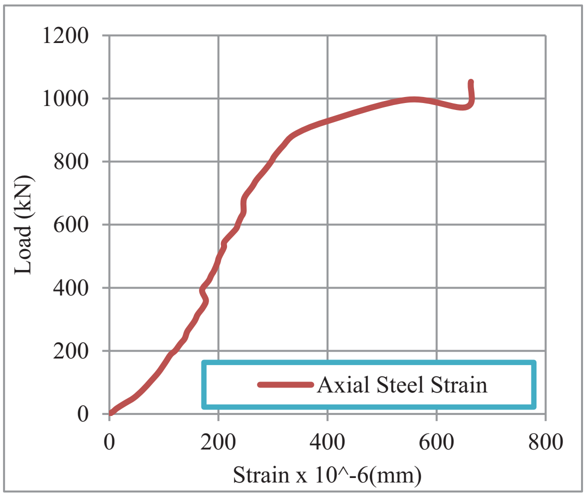


*(a) Conventional column*

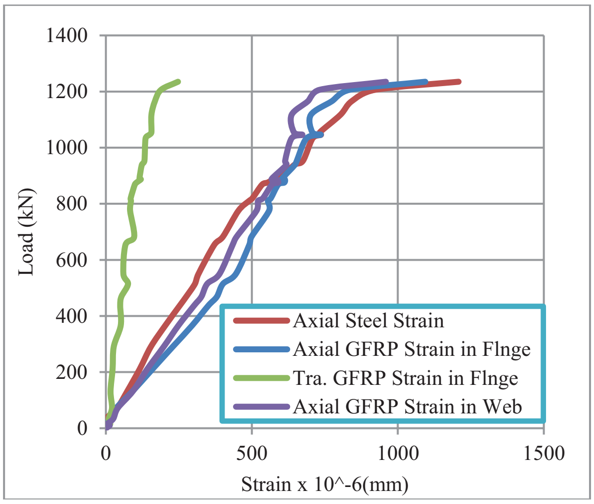


*(b) Composite column*

*Figure 9. The stress-strain curves of conventional and composite columns without firing*

## 4. THEORETICAL ANALYSIS

The ability of common structural analysis tools to predict the performance of the tested RC composite columns was investigated in order to provide practicing engineers with information on their respective reliability according to the different codes was considered.

The ultimate strength of the conventional RC columns is calculated at point failure, the theoretical ultimate strength or nominal strength of a short axially loaded column is determined quite accurately by the Egyptian Code of Practice (ECP-203) [13] and British Standard BS 8110-97 [14], the theoretical maximum load can be calculated by both the concrete and reinforcement contribute in bearing the axial load as the following;

$$P_n = 0.67 f_{cu}(A_g - A_{st}) + f_y A_{st} \qquad (1)$$

According to ACI 318-11 [15], the theoretical maximum load can be calculated as the contribution of both the concrete and the reinforcement in carrying the axial load;

$$P_n = 0.85 f'_c (A_g - A_{st}) + f_y A_{st} \qquad (2)$$

The maximum nominal axial load on a column is calculated from the following equation according to Eurocode [16];

$$P_n = \eta f'_c (A_g - A_{st}) + f_s A_{st} \qquad (3)$$

Where; $\eta = 1.0$ for $f'_c \leq 50$ MPa (4)

$\eta = 1.0 - (f'_c - 50)/200$ for $50 < f'_c \leq 90$ MPa (5)

$$f_s = \varepsilon_c E_s \qquad (6)$$

$\varepsilon_c = 2\%$ for $f'_c < 50$ MPa (7)

$\varepsilon_c(\%) = 2 + 0.085(f'_c - 50)^{0.53}$ for $f'_c \geq 50$ MPa (8)

The maximum nominal axial load on the column is calculated by the following equation according CSA A23.3-04 [17];

$$P_n = \alpha_1 \phi_c f'_c (A_g - A_{st}) + \phi_s f_y A_{st} \qquad (9)$$

$\alpha_1 = 0.85 - 0.0015 f'_c$ but not less than 0.67 (10)

By comparing between the experimental results and values calculated by the theoretical equation of the different codes, find that, the experimental and theoretical results calculated by Egyptian Code of Practice (ECP-203) [13], British Standard BS 8110-97 [14], and ACI 318-11 [15] is scientific research converge very closely for the axial load , indicating the strength and reliability of the findings obtained and showed similar results as observed by the experiment and no significant differences in axial loads were found as shown in Table 3. Therefore, the proposed equation to calculate the axial load of RC composite columns based on the Egyptian Code of Practice, and different Standard codes as following;

ECP-203 & BS $$P_n = 0.67 f_{cu}(A_g - A_{st}) + f_y A_{st} + 0.65 f_f A_f \quad (11)$$

ACI $$P_n = 0.85 f'_c (A_g - A_{st}) + f_y A_{st} + 0.65 f_f A_f \quad (12)$$

Eurocode $$P_n = \eta f'_c (A_g - A_{st}) + f_s A_{st} + 0.65 f_f A_f \quad (13)$$

CSA $$P_n = \alpha_1 \phi_c f'_c (A_g - A_{st}) + \phi_s f_y A_{st} + 0.65 f_f A_f \quad (14)$$

The reinforced concrete columns exposed to fire at 500 degrees, according to Eurocode 1991-1-2, section 3 [16], for the conventional reinforced concrete columns the reduction factor *kc,θ,* and *ky,θ,* to be applied to the compressive strength of concrete and the yield strength of steel and equal to 0.74 and 0.78 respectively. And it can be applied to composite columns, in addition to neglecting the resistance of GFRP due to the organic resin matrix used in GFRP compounds is melts at high temperature.

*Table 3. Comparison between experimental and theoretical results of composite columns*

| Specimen Code | Maximum load (kN) | | | | | $P_{Exp.}$ / $P_{Theo.}$ | | | |
|---|---|---|---|---|---|---|---|---|---|
| | $P_{exp.}$ | $P_{ECP\& BS}$ | $P_{ACI.}$ | $P_{EUR.}$ | $P_{CSA.}$ | ECP& BS | ACI | EUR | CSA |
| RCC | 1052.90 | 1043.04 | 1055.55 | 1129.69 | 1,005.50 | 1.01 | 1.00 | 0.93 | 1.05 |
| RCCGI-C | 1234.30 | 1232.74 | 1243.74 | 1299.72 | 1199.75 | 1.00 | 0.99 | 0.95 | 1.03 |
| RCC-F | 900.71 | ------- | ------- | 841.12 | ------- | ------- | ------- | 1.07 | ------ |
| RCCGI-C-F | 746.99 | -------- | -------- | 751.54 | -------- | -------- | -------- | 0.99 | ------ |

The theoretical calculations and the accuracy of the proposed equation according to different codes were able to accurately predict the load capacity of composite columns under vertical load.

## 5. NUMERICAL ANALYSIS.

The non-linear finite element analysis method, as well as, the finite element analysis by using ANSYS (R19) program considered. The columns behaved nonlinearly mainly as its component materials have nonlinearity due to elastic plastic steel reinforcement bars and the linear pseudo plastic and brittle behavior of the concrete. This analysis method is currently considered as the state of the art for analysing reinforced concrete structures. However, the use of this sophisticated tool is complicated by the need to select several control parameters, which are usually chosen based on previous experience in correlating the results of the finite element analysis to real experimental results similar to the ones to be analyzed.

In addition to reproducing the behavior of the tested columns without firing, the nonlinear analyses were performed in order to study, the effect of the concrete compressive strength, the effect of the steel compressive strength of steel, the effect of reinforcement ratio, and the effect of percentage of GFRP ratio of the composite columns. The analysis was performed using the finite element package ANSYS [18].

### 5.1 Modeling

The solid element, SOLID65, was used to model the concrete, the 3D spar Link180 element was used to model the steel bars and the solid element, Solid185, was used to model the GFRP I-section and steel plates at the supports for the columns. The model of the verification column is shown in Fig. 10.

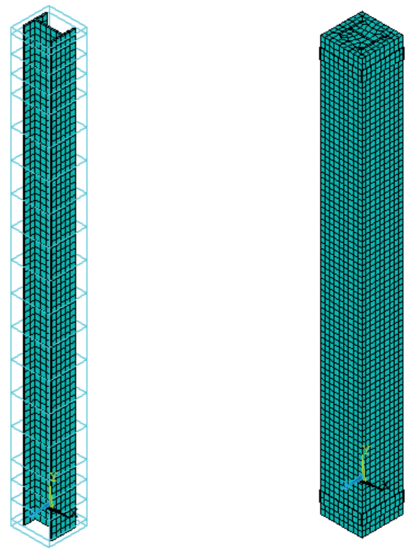

*(a) Link elements for steel bars and GFRP I-section* *(b) Solid elements for concrete & steel plates*

*Figure 10. The model of the column used in the nonlinear analysis*

## 5.2 Material properties

Equation (1), proposed by MacGregor [19], is used to represent the uniaxial compressive stress-strain relationship for concrete.

$$f = \frac{E_c \varepsilon}{1 + \left(\frac{\varepsilon}{\varepsilon_o}\right)^2} \qquad (15)$$

This equation has been used to plot the multi-linear isotropic stress-strain curve for concrete from 0.3fc' to the ultimate compressive strength, *0.3fc'*.the Elastic modulus is defined as 0.3fc', and calculated in the linear region. While elastic plastic uniaxial stress- strain model is used to model reinforcing steel. In addition, the modulus of elasticity and the tensile strength of concrete are calculated using the same specifications. The stress-strain curves of steel bars were presented according to ECP 203 Code of Practice [13]. GFRP was assumed to be linear, elastic and orthotropic material, and the material properties based on provided by the manufacturer were input to the model. The elastic plastic uniaxial stress -strain model given in ECP 203 Code of Practice [13] was used to model steel.

## 5.3 Validation of the numerical nonlinear model

For the validation of the ANSYS model for the RC composite columns, the determination of the parameters controlling the details of the concrete material model of SOLID65, such as the tensile stiffening and the shear retention across cracks of the reinforced concrete, were determined empirically by finding the values achieving the best fit of the calculated stress - strain curve of the RC composite column with the experimental one. The best numerical curve and the experimental curve are given in Fig. 11. It can be seen that, in general, the numerical curve is matching with the experimental one. However, it is relatively less stiff than the experimental curve.

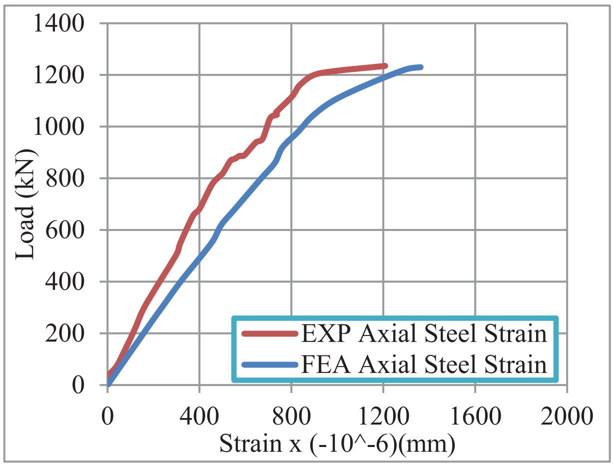


*(a) Axial strain of steel bars*

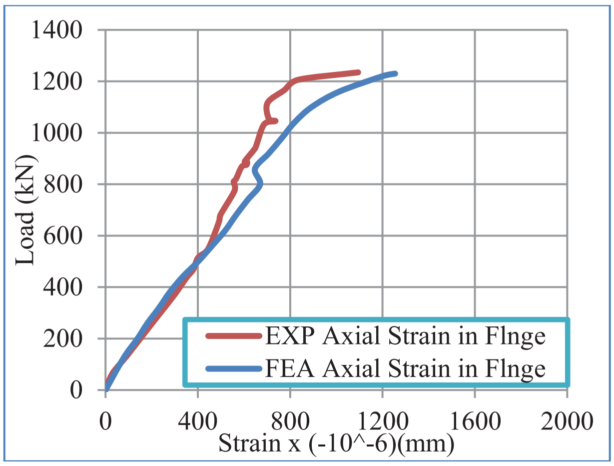


*(b) Axial strain of GFRP I-section*

*Figure 11. The experimental and numerical stress-strain curves of verification column*

### 5.4 Parametric study

After verification of the finite element model, four parameters were further investigated for the conventional RC columns and the RC composite columns: -

(i) Effect of the compressive strength of concrete,
(ii) Effect of the yield strength of steel,
(iii) Effect of reinforcement ratio, and
(iv) Effect of percentage of GFRP I-section ratio of the RC composite columns.

Through it, the proposed equation for calculating the axial load of RC composite columns can be verified.

#### *5.4.1 Effect of concrete compressive strength*

To investigate the influence of the normal and high compressive strength of concrete on the bearing capacity of columns, nine analyses were performed for concrete strengths ranging from 20 MPa to 100 MPa to account for this parameter in this study for conventional RC columns and RC composite columns.

The theoretical calculated maximum axial loads by the Egyptian Code of Practice (ECP-203) [13] and British Standard BS 8110-97 [14] and the numerical calculated maximum axial loads by finite element analysis are given in Table 4 and Fig. 12. It is noted that the calculated maximum axial loads closely agree with the numerical values and doesn't exceed 2% and 4% for conventional RC columns and RC composite columns respectively, except when the compressive strength of concrete is equal to 20 MPa, the maximum axial loads calculated by finite element analysis is 8% increase about the calculated maximum axial loads by the proposed equation for RC composite columns.

*Table 4. Effect of concrete compressive strength on theoretical and numerical maximum axial loads*

| No. | Concrete compressive strength ($F_{cu}$) (MPa) | Conventional columns | | | Composite columns | | |
|---|---|---|---|---|---|---|---|
| | | $P_{Theo.}$ (kN) | $P_{FEM}$ (kN) | $P_{FEM}/P_{Theo.}$ | $P_{Pequ.}$ (kN) | $P_{FEM}$ (kN) | $P_{FEM}/P_{Pequ.}$ |
| CSC1 | 20 | 543.52 | 542.00 | 1.00 | 816.25 | 881.00 | 1.08 |
| CSC2 | 30 | 712.88 | 701.00 | 0.98 | 976.44 | 1020.00 | 1.04 |
| CSC3 | 40 | 882.24 | 880.00 | 1.00 | 1136.63 | 1160.00 | 1.02 |
| CSC4 | 50 | 1051.61 | 1050.00 | 1.00 | 1296.81 | 1340.00 | 1.03 |
| CSC5 | 60 | 1220.97 | 1212.00 | 0.99 | 1457.00 | 1470.00 | 1.01 |
| CSC6 | 70 | 1390.33 | 1382.00 | 0.99 | 1617.19 | 1580.00 | 0.98 |
| CSC7 | 80 | 1559.69 | 1530.00 | 0.98 | 1777.38 | 1760.00 | 0.99 |
| CSC8 | 90 | 1729.06 | 1721.00 | 1.00 | 1937.56 | 1970.00 | 1.02 |
| CSC9 | 100 | 1898.42 | 1921.00 | 1.01 | 2097.75 | 2180.00 | 1.04 |

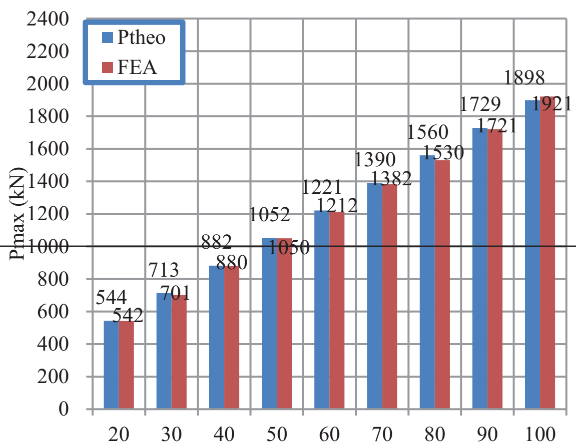


*(a) Conventional columns*

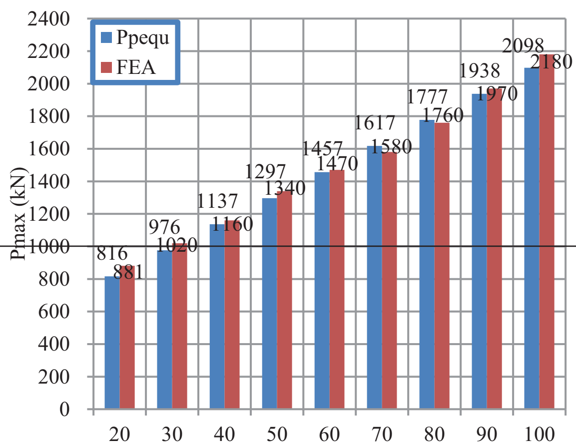


*(b) Composite columns*

*Figure 12. Effect of concrete compressive strength on theoretical and numerical maximum axial loads*

Fig. 13 shows that the relationship between compressive strength of concrete and axial load of the conventional RC columns and RC composite columns. It can be seen that, the axial load increases linearly proportionally with the increase of compressive strength of concrete.

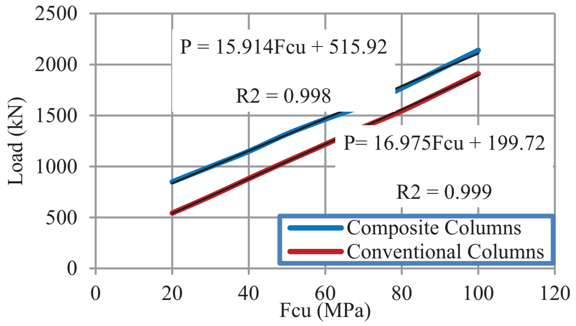


*Figure 13. Relationship between concrete compressive strength and axial load*

### *5.4.2 Effect of yield strength of steel*

The yield strength of steel does not significantly affect the axial load capacity of conventional RC columns as shown in Table 5 and doesn't apply to RC composite columns; all stresses in the longitudinal reinforcement have been monitored to theoretical specimens by finite element analysis of the previous parameters. It is noted that the maximum stress in steel bars are less than 300 MPa for compressive strength of concrete up to 50 MPa and the stress in steel bars equal to 525.33 MPa of for high compressive strength of concrete at 100 MPa respectively. Therefore, the Eurocode [16] takes the stress value in the longitudinal steel is equal to the young's modulus of steel multiplied by the strain of concrete when reaching the maximum strength.

*Table 5. Effect of stress in steel bars at the different compressive strength of concrete*

| No. | Compressive strength ($F_{cu}$) (MPa) | Conventional columns | |
|---|---|---|---|
| | | $P_{FEM}$ (kN) | Stress in steel (MPa) |
| CSS1 | 20 | 542.00 | 194.67 |
| CSS2 | 30 | 701.00 | 226.91 |
| CSS3 | 40 | 880.00 | 263.17 |
| CSS4 | 50 | 1050.00 | 288.16 |
| CSS5 | 60 | 1212.00 | 333.95 |
| CSS6 | 70 | 1382.00 | 392.95 |
| CSS7 | 80 | 1530.00 | 428.55 |
| CSS8 | 90 | 1721.00 | 473.61 |
| CSS9 | 100 | 1921.00 | 525.33 |

### *5.4.3 Effect of reinforcement ratio*

To study the influence of the longitudinal reinforcement ratio (ρ) on the behavior of conventional RC columns and RC composite columns, the analyses were performed for four different values 0.79%, 1.23%, 1.77%, and 3.14% by using diameters of 8 mm, 10 mm, 12 mm, and 16 mm respectively, with concrete compressive strength equal to 40 MPa and steel compressive strength equal to 400 MPa.

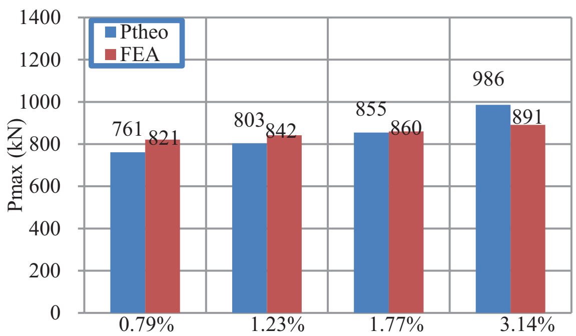


*(a) Conventional columns*

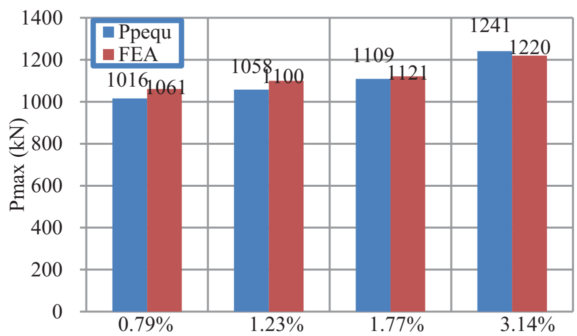


*(b) Composite columns*

*Figure 14. Effect of the reinforcement ratio on theoretical and numerical maximum axial loads*

The theoretical calculated maximum axial loads and the numerical maximum axial loads are shown Fig. 14 and given Table 6. It is noted that the calculated maximum axial loads are close the numerical values and don't exceed 4.48% for RC composite columns. While, the theoretical calculated maximum axial loads increase when the reinforcement ratio is less than 1.25% and decrease when the reinforcement ratio is greater than 2.00%. Therefore, it is possible to reconsider the calculation of the value of axial load resulting from the compressive stress in the reinforcing steel.

*Table 6. Effect of reinforcement ratio on theoretical and numerical maximum axial loads*

| No. | RFT. Ratio (%) | Conventional columns | | | Composite columns | | |
|---|---|---|---|---|---|---|---|
| | | $P_{Theo.}$ (kN) | $P_{FEM}$ (kN) | $P_{FEM}/P_{Theo.}$ | $P_{pequ.}$ (kN) | $P_{FEM}$ (kN) | $P_{FEM}/P_{Pequ.}$ |
| RS1 | 0.79 | 761.15 | 821.00 | 1.08 | 1015.53 | 1061.00 | 1.04 |
| RS2 | 1.23 | 803.37 | 842.00 | 1.05 | 1057.76 | 1100.00 | 1.04 |
| RS3 | 1.77 | 854.98 | 860.00 | 1.01 | 1109.36 | 1121.00 | 1.01 |
| RS4 | 3.14 | 986.35 | 891.00 | 0.90 | 1240.73 | 1220.00 | 0.98 |

Fig. 15 shows that the relationship between reinforcement ratio and axial load of the conventional RC columns and RC composite columns. It can be seen that, the numerical maximum axial load increases linearly proportionally with the increase of reinforcement ratio up to approximately 3% and then decreases for conventional RC columns, while the rate of increase is linear for RC composite columns.

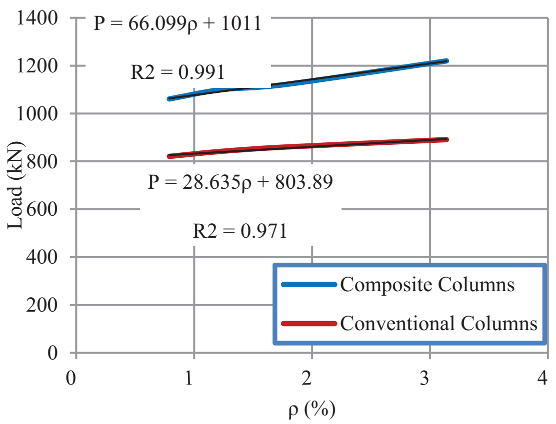


*Figure 15. Relationship between reinforcement ratio and axial load*

### *5.4.4 Effect of GFRP ratio*

In order to investigate the influence of the GFRP ratio on the behavior of RC composite columns, the analyses were performed for twelve different values ranging from 2.03% to 17.18% by using two different shapes of GFRP sections, GFRP sections were shaped as flat plates, and I-shape respectively, concrete compressive strength was equal to 40 MPa and steel compressive strength was equal to 400 MPa. The theoretical calculated maximum axial loads and the numerical maximum axial loads are given in Table 7 and Fig. 16. It can be seen that the calculated maximum axial loads are close to the numerical values for RC composite columns with GFRP ratio up to 4% and 8% for flat plates and I-shape respectively. While, the numerical maximum axial loads are almost constant at GFRP ratio more than 4% and 8% for flat plates and I-shape respectively. Therefore, the proposed equation for calculating of the axial load of RC composite columns is satisfactory at GFRP ratios less than 4% and 8% for flat plates and I-shape respectively.

*Table 7. Effect of GFRP ratio on theoretical and numerical maximum axial loads*

| No. | GFRP section | GFRP dimensions (mm) | GFRP I-section ratio (%) | $P_{Equ}$ (kN) | $P_{FEM}$ (kN) | $P_{FEM}$ / $P_{PEqu}$ | Stress in steel (Mpa) | Stress in GFRP (MPa) |
|---|---|---|---|---|---|---|---|---|
| RGFRP-P1 | Flat Plate | 89x5.5 | 2.03 | 899.91 | 935.00 | 1.04 | 349.05 | 181.41 |
| RGFRP-P2 | | 84x8 | 2.88 | 940.08 | 998.75 | 1.06 | 400.00 | 212.00 |
| RGFRP-P3 | | 80x10 | 3.52 | 970.55 | 1040.00 | 1.07 | 400.00 | 213.09 |
| RGFRP-P4 | | 76x12 | 4.13 | 999.52 | 995.00 | 1.00 | 362.04 | 166.67 |
| RGFRP-P5 | | 70x15 | 4.98 | 1040.20 | 980.00 | 0.94 | 359.82 | 140.53 |
| RGFRP-P6 | | 60x20 | 6.25 | 1058.35 | 980.00 | 0.93 | 301.61 | 116.70 |
| RGFRP-I1 | I-section | 100x80x5.5 | 5.35 | 1057.76 | 1100.00 | 1.04 | 400.00 | 292.43 |
| RGFRP-I2 | | 100x80x8 | 7.63 | 1165.96 | 1107.50 | 0.95 | 400.00 | 199.97 |
| RGFRP-I3 | | 100x80x10 | 9.38 | 1249.17 | 1178.75 | 0.94 | 400.00 | 321.55 |
| RGFRP-I4 | | 100x80x12 | 11.06 | 1329.42 | 1195.00 | 0.90 | 400.00 | 205.90 |
| RGFRP-I5 | | 100x80x15 | 13.48 | 1444.21 | 1197.50 | 0.83 | 400.00 | 257.64 |
| RGFRP-I6 | | 100x80x20 | 17.18 | 1578.45 | 1210 | 0.77 | 338.93 | 147.14 |

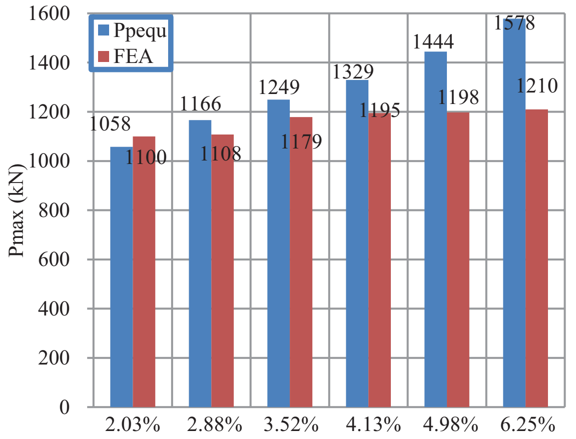


(a) Flat Plate shape

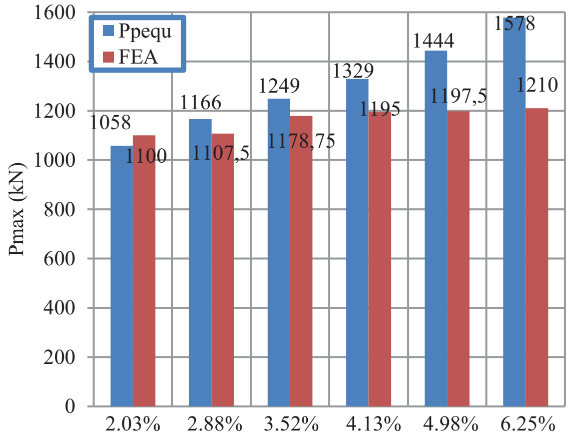


(b) I-Shape

*Figure 16. Effect of the GFRP ratio on the theoretical and numerical maximum axial loads*

The resistance of the RC composite columns is increases as the surface area of the GFRP increases and the homogeneity inside the concrete section.

## 6. CONCLUSIONS

From the experimental, theoretical and numerical results on the axial load behavior of the proposed composite columns reinforced with Glass Fibre Reinforced Polymer (GFRP) profiles and longitudinal steel bars, the following conclusions can be drawn:

1. Glass Fiber Reinforced Polymer (GFRP) I-profile concrete composite columns have proven to be structurally efficient elements with high axial load capacity.
2. Compared to the conventional RC columns, the RC composite columns with internal (GFRP) I-profile showed 17% higher ultimate capacity, and less displacement at the same loading levels.
3. The axial load is reduced by about 14% and 39% for conventional RC column and RC composite column respectively exposed to fire at a temperature of 500 C° to one and half hour.
4. The proposed theoretical equation accurately predicts the axial load calculation of RC composite columns and should take the reduction factor of the compressive strength of GFRP I-section equal to 0.65.

5. The numerical model predictions were close to the experimental results. In a wide range of load -bearing capacity values investigated, less than 1.5% error was observed between the compressive strength predicted by the finite element analysis and the experimental results.
6. The Results indicated that the finite element model used in this study was able to predict the axial load of RC composite columns with reasonable accuracy.
7. The numerical results indicated that the axial load capacity of the RC composite columns increased with increasing GFRP ratio up to 4 % and 8% for flat plate and I-shape respectively.
8. The axial load increases with an increase of the compressive strength of concrete, longitudinal reinforcement ratio for conventional RC columns and RC composite columns.
9. The axial load doesn't increase proportionally with the increasing stress of the rebar, where the effective stress of the rebar doesn't exceed 300 MPa, and 525 MPa for compressive strength of concrete up to 50 MPa and high compressive strength of concrete up to 100 MPa respectively for conventional RC columns.

## REFERENCES


1. **Hadi M., Youssef J.** Experimental Investigation of GFRP-Reinforced and GFRP-Encased Square Concrete Specimens under Axial and Eccentric Load, and Four-Point Bending Test // Journal of Composites for Construction, 2016.
2. **Jing C., Zhao L., Wu T., Li.** Experimental and Numerical Simulation of Reinforced Concrete-Filled Square GFRP Tubular Columns under Axial Compression // Materials 17, 2024, 2595.
3. **Hadi M., Wang W., Sheikh M.** Axial compressive behavior of GFRP tube reinforced concrete columns // Construction and Building Materials 81, 2015, 198-207.
4. **Tomblin J., Barbero E.** Local buckling experiments on FRP columns // Thin Walled Sruct. 18(2), 1994, 97-116.
5. **Harvey J.** A reinforced plastic footbridge, Aberfeldy, UK // Structural Engineering International, 4/93, 2018, 229-232.
6. **Robert L., Zouheir A., Short vs.** Long column behavior of pultruted glass-fiber reinforced polymer composites // Construction and Building Materials 15, 2001, 369-378.
7. **Lei X., Yu B., Yujun Q., Hao W.** Pultruded GFRP Square Hollow Columns with Bolted Sleeve Joints under Eccentric Compression //https://www.elsevier.com/userlicense/1.0/, 2018.
8. **Srinath T.** Buckling and Bonding Behavior of Glass Fiber Reinforced Epoxy Resin Composite Column // International Journal of Electrical Engineering and Technology (IJEET), Vol. 11, 2020, 219-224.
9. **Yunjun Q., Lei X., Yu B., Weiqing Liu., Hao W.** Axial Compression Behaviors of Pultruted GFRP-Wood Composite Columns // www.mdpi.com, journal/sensors, 2019.
10. **Aydin F.** Effects of various temperatures on the mechanical strength of GFRP box profiles // Construction and Building Materials 127, 2016, 843-849.
11. **OPCT**. Fiberglass Products Company, 398 Kaiyuan Road, Jizhou District, Hengshui City, Hebei Province, China // www.Chopct.com.
12. **Hassooni A., Zaidee S.** Behavior and Strength of Composite Columns under the Impact of Uniaxial Compression Loading // Engineering Technology and Applied Science Research, Vol. 12, No. 4, 2022, 8843-8849.
13. **Egyptian code** for design and construction of reinforced concrete structures, Housing and Building National Research Center.

Ministry of Housing, Utilities and Urban Planning, Giza, Egypt, ECP 203-2020.
14. **British Standards Institution.** Structural use of concrete, Part 1: code of practice for design and construction. British Standards Institution, London, BS811O - 1997.
15. **ACI Committee.** American Concrete Institute, & International Organization for Standardization, Building code requirements for structural concrete and commentary. American Concrete Institute (ACI 318-11).
16. **European Standard**. Design of concrete structures – part 1-1: General rules and rules for buildings. CEN, Brüssel, EN 1992-1-1, 2011.
17. **CSA Code Canadian** Standards Association for Design of Concrete Structures, Consolidated Mailing, Canada CSA. A23.3-04, 2004.
18. **ANSYS.** "ANSYS Help", Release 19, Copyright 2012.
19. **MacGregor G.** Reinforced Concrete Mechanics and Design", Prentice-Hall, Inc., Englewood Cliffs, NJ, 1992.

## СПИСОК ЛИТЕРАТУРЫ

1. **Hadi M., Youssef J.** Experimental Investigation of GFRP-Reinforced and GFRP-Encased Square Concrete Specimens under Axial and Eccentric Load, and Four-Point Bending Test // Journal of Composites for Construction, 2016.
2. **Jing C., Zhao L., Wu T., Li.** Experimental and Numerical Simulation of Reinforced Concrete-Filled Square GFRP Tubular Columns under Axial Compression // Materials 17, 2024, 2595.
3. **Hadi M., Wang W., Sheikh M.** Axial compressive behavior of GFRP tube reinforced concrete columns // Construction and Building Materials 81, 2015, 198-207.
4. **Tomblin J., Barbero E.** Local buckling experiments on FRP columns // Thin Walled Sruct. 18(2), 1994, 97-116.
5. **Harvey J.** A reinforced plastic footbridge, Aberfeldy, UK // Structural Engineering International, 4/93, 2018, 229-232.
6. **Robert L., Zouheir A., Short vs.** Long column behavior of pultruted glass-fiber reinforced polymer composites // Construction and Building Materials 15, 2001, 369-378.
7. **Lei X., Yu B., Yujun Q., Hao W.** Pultruded GFRP Square Hollow Columns with Bolted Sleeve Joints under Eccentric Compression //https://www.elsevier.com/userlicense/1.0/, 2018.
8. **Srinath T.** Buckling and Bonding Behavior of Glass Fiber Reinforced Epoxy Resin Composite Column // International Journal of Electrical Engineering and Technology (IJEET), Vol. 11, 2020, 219-224.
9. **Yunjun Q., Lei X., Yu B., Weiqing Liu., Hao W.** Axial Compression Behaviors of Pultruted GFRP-Wood Composite Columns // www.mdpi.com, journal/sensors, 2019.
10. **Aydin F.** Effects of various temperatures on the mechanical strength of GFRP box profiles // Construction and Building Materials 127, 2016, 843-849.
11. **OPCT**. Fiberglass Products Company, 398 Kaiyuan Road, Jizhou District, Hengshui City, Hebei Province, China // www.Chopct.com.
12. **Hassooni A., Zaidee S.** Behavior and Strength of Composite Columns under the Impact of Uniaxial Compression Loading // Engineering Technology and Applied Science Research, Vol. 12, No. 4, 2022, 8843-8849.
13. **Egyptian code** for design and construction of reinforced concrete structures, Housing and Building National Research Center. Ministry of Housing, Utilities and Urban Planning, Giza, Egypt, ECP 203-2020.
14. **British Standards Institution.** Structural use of concrete, Part 1: code of practice for design and construction. British Standards Institution, London, BS811O - 1997.

15. **ACI Committee.** American Concrete Institute, & International Organization for Standardization, Building code requirements for structural concrete and commentary. American Concrete Institute (ACI 318-11).
16. **European Standard**. Design of concrete structures – part 1-1: General rules and rules for buildings. CEN, Brüssel, EN 1992-1-1, 2011.
17. **CSA Code Canadian** Standards Association for Design of Concrete Structures, Consolidated Mailing, Canada CSA. A23.3-04, 2004.
18. **ANSYS.** “ANSYS Help”, Release 19, Copyright 2012.
19. **MacGregor G.** Reinforced Concrete Mechanics and Design", Prentice-Hall, Inc., Englewood Cliffs, NJ, 1992.

---

*Mohammed Abdel-Rahman M. Khalil M.Sc,* Faculty of Engineering, Helwan University, Egypt. E-mail: mamkhalil@m-eng.helwan.edu.eg

*Mohammed M. Salem,* Assistant Professor of Structure Engineering, Faculty of Engineering, Mataria, Helwan University, Egypt. E-mail: Mohamedsalem@m-eng.helwan.edu.eg

*Ata El-Kariem Shoeib Soliman,* Professor of Reinforced Concrete Structures, Faculty of Engineering, Mataria, Helwan University, Egypt. E-mail: atta_alsayed@m-eng.helwan.edu.eg.

*Alaa Gamal Sheriff*, Professor of Reinforced Concrete Structures, Faculty of Engineering, Mataria, Helwan University, Egypt. E-mail: agbsherif@gmail.com

*Мохаммед Абдель-Рахман М. Халил*, магистр технических наук, инженерный факультет, Университет Хелуан, Египет. E-mail: mamkhalil@m-eng.helwan.edu.eg

*Мохаммед М. Салем*, доцент кафедры инженерных конструкций, инженерный факультет, Матария, Хелуанский университет, Египет. E-mail: Mohamedsalem@m-eng.helwan.edu.eg

*Ата Эль-Карим Шоиб Солиман*, профессор кафедры железобетонных конструкций, инженерный факультет, Матария, Хелуанский университет, Египет. E-mail: atta_alsayed@m-eng.helwan.edu.eg

*Алаа Гамаль Шериф,* профессор кафедры железобетонных конструкций, инженерный факультет, Матария, Хелуанский университет, Египет. E-mail: agbsherif@gmail.com